Research Square

Preprints are preliminary reports that have not undergone peer review.
They should not be considered conclusive, used to inform clinical practice,
or referenced by the media as validated information.

Rainfall structure and modelled surface drying in relation to crop response in degradation prone rainfed lands of eastern Sudan

Mohamed Abaker
Sudan University of Science and Technology
Jamal Elfaki
jamal.elfaki@sustech.edu

Sudan University of Science and Technology

Research Article

Keywords: land degradation, rainfall structure, surface drying, rainfed agriculture, CHIRPS

Posted Date: August 27th, 2026

DOI: https://doi.org/10.21203/rs.3.rs-10477376/v1

License: This work is licensed under a Creative Commons Attribution 4.0 International License.
Read Full License

Additional Declarations: No competing interests reported.

Rainfall structure and modelled surface drying in relation to crop response in degradation prone rainfed lands of eastern Sudan

Mohamed Abaker[1] and Jamal Elfaki[1*]

[1] Department of Soil and Water Science, College of Agricultural Studies, Sudan University of Science and Technology, Khartoum, Sudan

[*]Corresponding author: jamal.elfaki@sustech.edu

Abstract

Dryland croplands that depend on seasonal rainfall are vulnerable to surface drying and unstable production when rainfall is delayed, interrupted, or concentrated in a few events. This study assessed long-term rainfall-structure risk, modelled surface drying, and crop response in degradation-prone rainfed agricultural lands of Gedaref State, eastern Sudan, during 1982–2020. Daily CHIRPS rainfall, monthly FLDAS Noah surface soil moisture, and annual sorghum and sesame records were analysed. CHIRPS seasonal rainfall showed moderate agreement with the station record ($r = 0.625$), with a mean bias of −77.5 mm and an RMSE of 130.0 mm. A Daily Rainfall-Structure Risk Index (DRSRI) was developed from seasonal rainfall deficit, maximum June–September consecutive dry days, rainfall-onset delay, and the share of seasonal rainfall received during the five wettest days. The first principal component explained 60.4% of the standardised variance. Higher DRSRI values were associated with lower modelled surface soil moisture ($r = −0.776$, $p < 0.001$), indicating greater surface-drying exposure in years with unfavourable rainfall structure. In rolling-origin evaluation, the four rainfall variables slightly outperformed seasonal rainfall alone, although the difference was not significant, and DRSRI alone predicted less accurately than seasonal rainfall (RMSE 0.681 versus 0.554). DRSRI was also associated with lower detrended sorghum harvested-area ratio anomalies ($r = −0.448$; FDR-adjusted $p = 0.015$), while yield associations were not significant after correction. Eight compound-risk years showed lower surface soil-moisture and sorghum harvested-area ratio anomalies than other years. Daily rainfall-structure indicators can support regional screening of surface drying and agricultural exposure in dryland farming landscapes susceptible to degradation.

Keywords: land degradation; rainfall structure; surface drying; rainfed agriculture; CHIRPS.

1. Introduction

1.1 Rainfall amount and within-season structure

Agricultural drought in rainfed systems is often described using seasonal rainfall totals or standardised precipitation indices. These measures describe the seasonal amount, but not when rainfall starts, how often it is interrupted, or how much of it falls in a few events. Two seasons may receive similar totals while differing in the number of rainy days, the length of dry periods, and the share of rainfall delivered by a few large events (Palmer, 1965; McKee et al., 1993; Mishra and Singh, 2010; Zargar et al., 2011). Daily rainfall data are therefore needed to examine the wetting and drying sequence experienced by soil and crops during the growing season (Alexander et al., 2006; Zhang et al., 2011).

The effect of rainfall on rainfed agriculture depends on timing and continuity as much as on total amount. Repeated rainfall can keep the surface layer moist and support crop establishment. Long gaps between events can expose crops and bare soil to water stress, even when the seasonal total is not very low. Rainfall that is concentrated in a few events may also leave long dry intervals between wetting periods. In cultivated dryland areas, these patterns matter because surface drying, poor establishment, and unstable production are part of the wider pressure on land condition. Crop response is also shaped by growth stage, soil condition, cultivar, and management (Allen et al., 1998; Rockström et al., 2002; Rockström, 2003; Rockström et al., 2010; Schlenker and Lobell, 2010; Lobell and Burke, 2010; Lobell et al., 2011; Sultan et al., 2013; IPCC, 2022).

1.2 Daily rainfall structure in rainfed lands of Gedaref

Gedaref State is one of the main mechanised rainfed farming regions in Sudan. Sorghum and sesame are widely grown on the clay plains. Cultivation has also expanded into more marginal areas, which has increased exposure to rainfall variability and land degradation (Sulieman and Buchroithner, 2009). In this setting, rainfall structure is relevant to land management as well as climate analysis. A season with delayed onset, a long dry spell, or rainfall concentrated in a few events can increase surface drying and reduce the reliability of crop production.

The first isolated rainfall event does not always mark the effective start of the growing season. A more useful onset measure is based on rainfall accumulated over several consecutive days. Daily records also allow direct calculation of consecutive dry days and the degree to which seasonal rainfall is concentrated in a few large events (Stern et al., 1981; Sivakumar, 1988, 1992; Ati et al., 2002; Usman and Reason, 2004; Marteau et al., 2011; Dunning et al., 2016). These indicators describe the sequence of wetting and drying that cannot be seen from seasonal totals alone.

Rainfall over eastern Africa can vary strongly from place to place, especially during seasons dominated by local convective storms. Gridded rainfall products must therefore be compared with available station observations and interpreted according to the spatial area they represent (Dinku et al., 2007; Nicholson, 2017; Gebrechorkos et al., 2019). In this study, CHIRPS

rainfall and FLDAS soil moisture were averaged over the administrative boundary of Gedaref State. The resulting series describe regional conditions across the state. They should not be read as measurements for individual farms or fields.

Sesame production in Gedaref is also affected by factors that are not represented by rainfall indicators. These include access to finance and inputs, labour requirements at harvest, capsule shattering, pests and diseases, transport costs, and post-harvest handling (Babiker, 2010; United Nations Industrial Development Organization [UNIDO], 2017; Ibrahim and Muhieldeen, 2018; Abdalla, 2022). These factors can weaken the year-to-year relationship between rainfall and administratively reported sesame yield. Crop records were therefore used here as broad agricultural response indicators, not as a direct measure of rainfall effect alone.

1.3 Modelled surface soil moisture as a response layer

Long-term field measurements of soil moisture are not available for Gedaref. FLDAS provides a continuous modelled soil-moisture record based on the Noah land-surface model and was developed for monitoring water conditions in regions where ground observations are limited (Ek et al., 2003; Rodell et al., 2004; McNally et al., 2017; Arsenault et al., 2020). The 0–10 cm layer was used to examine whether years with unfavourable rainfall structure also had lower modelled surface moisture. Surface soil moisture represents the upper part of the soil-water system and is closely linked to rainfall, evaporation, runoff, and land–atmosphere exchange (Seneviratne et al., 2010).

The surface layer is important in rainfed land management because it responds quickly to rainfall and drying. Low surface moisture can affect crop establishment, bare-soil exposure, runoff behaviour, and the period during which the soil remains wet after rainfall. The 0–10 cm FLDAS layer was therefore used to check whether poor rainfall structure coincided with lower surface moisture across Gedaref.

The FLDAS product used in this study is partly driven by CHIRPS rainfall. The relationship between rainfall indicators and FLDAS soil moisture was therefore treated as a consistency assessment between rainfall forcing and modelled surface response, rather than as independent validation. Independent satellite products or field soil-moisture observations would be needed for a fully external assessment (Entekhabi et al., 2010; Dorigo et al., 2017; Gruber et al., 2019, 2020).

1.4 Study objectives

This study examined long-term rainfall-structure risk, modelled surface drying, and crop response in rainfed agricultural lands of Gedaref State during 1982–2020. The analysis focused on whether daily rainfall information can reveal forms of seasonal risk that are not captured by rainfall totals alone. It first described the main within-season rainfall features, including seasonal amount, onset timing, consecutive dry days, and rainfall concentration, and compared CHIRPS rainfall with the available station record to clarify the level of agreement between the gridded and observed rainfall data.

The study then developed a rainfall-only Daily Rainfall-Structure Risk Index from the main within-season rainfall indicators and examined whether this index was stable through time and consistent with modelled FLDAS surface soil moisture. The index and its component variables were also assessed against detrended sorghum and sesame records to determine whether years with unfavourable rainfall structure were associated with weaker agricultural response. Finally, the study identified years in which low rainfall, delayed onset, long dry spells, and rainfall concentration occurred together, and assessed whether daily rainfall-structure indicators can support regional screening of surface drying and agricultural exposure in dryland farming areas susceptible to degradation.

The study was designed as a regional analysis. It does not diagnose conditions at individual farms. Its purpose is to show whether daily rainfall structure can provide practical information for interpreting surface drying and agricultural exposure in rainfed lands where long-term soil-moisture observations are limited.

2. Materials and methods

2.1 Study area and spatial support

Gedaref State lies in eastern Sudan along the border with Ethiopia. It is one of the country's main rainfed farming areas, where sorghum and sesame are grown mainly on clay plains under a short and strongly seasonal rainfall regime. Most rainfall is received during the boreal summer, and crop production depends largely on rainfall received between June and September. Rainfall before and after this main period also affects soil wetting, crop establishment, and the length of dry intervals within the growing season. Here, degradation-prone refers to the expansion of mechanised cultivation into marginal clay plains and to the documented exposure of Gedaref to rainfall variability and land degradation (Sulieman and Buchroithner, 2009).

The analysis used the full administrative boundary of Gedaref State as the spatial support. Figure 1 shows the state localities, a reference point near Gedaref city, and the approximate grid-cell sizes of the CHIRPS and FLDAS products. No cropland or soil mask was applied. The extracted rainfall and soil-moisture series therefore represent state-level conditions used for regional screening of rainfall-structure risk and modelled surface drying. They should not be interpreted as measurements for individual farms, soil units, or cropped fields.

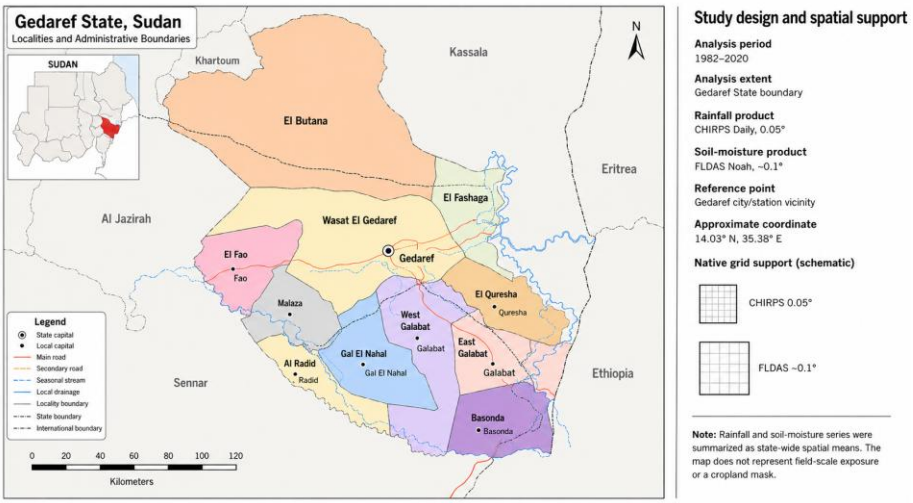


Figure 1. Location of Gedaref State and the spatial extent used in the analysis. The reference point indicates the approximate location of Gedaref city. The CHIRPS and FLDAS grid cells are shown schematically to illustrate the difference in their spatial resolutions.

Figure 2 summarises the analytical framework used in the study.

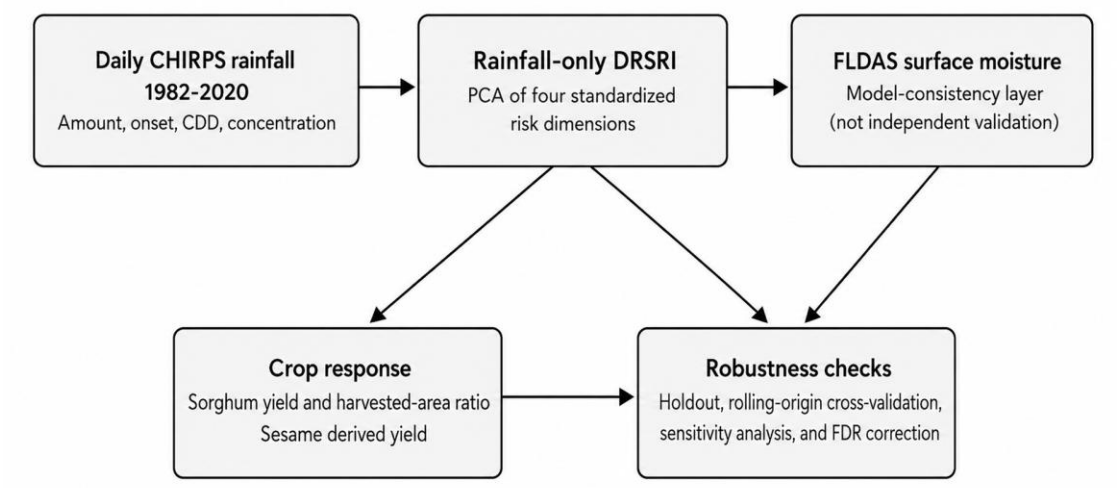


Figure 2. Analytical framework used in the study. DRSRI was derived only from rainfall variables. FLDAS surface soil moisture was used as a modelled surface-drying response layer, while crop records were used as broad agricultural response indicators. DRSRI, Daily Rainfall-Structure Risk Index; CDD, consecutive dry days; FDR, false discovery rate.

2.2 Data sources and harmonisation

All analyses covered the common period from 1982 to 2020. Daily CHIRPS rainfall (Funk et al., 2015) and monthly FLDAS Noah soil moisture (McNally et al., 2017; Arsenault et al., 2020) were obtained through Google Earth Engine. CHIRPS was accessed from UCSB-CHG/CHIRPS/DAILY, and FLDAS was accessed from NASA/FLDAS/NOAH01/C/GL/M/V001. For each date, the mean value of the grid cells intersecting the Gedaref State boundary was extracted. This kept the rainfall and soil-moisture products on the same state-level spatial support used for the regional analysis.

The extracted records contained 14,245 daily CHIRPS observations and 468 monthly FLDAS observations. Dates were checked for duplication, missing periods, negative values, and incomplete years before the annual indicators were calculated.

Monthly station rainfall records and annual sorghum and sesame statistics were obtained from the Gedaref State Ministry of Production and Economic Resources and the Mechanized Farming Corporation. The station rainfall record was used to evaluate the CHIRPS rainfall series. The crop records were used as administrative response data to examine broad agricultural exposure to rainfall-structure risk. The rainfall column included in the sesame record was not used because it was not consistent with the calendar years. All rainfall analyses were based on CHIRPS or the separate station archive (Gedaref State Ministry of Production and Economic Resources, n.d.-a, n.d.-b, n.d.-c).

The datasets, their analytical roles, and their principal limitations are summarised in Table 1.

Table 1. Data sources, analytical roles, and main limitations.

Dataset	Temporal and spatial resolution	Period	Analytical role	Main limitation
CHIRPS daily rainfall	Daily; 0.05°	1982–2020	Seasonal rainfall, onset, consecutive dry days, and rainfall concentration	A state-wide mean smooths localised rainfall events and dry spells
FLDAS Noah soil moisture	Monthly; approximately 0.1°	1982–2020	Modelled surface-drying response layer	Partly forced by CHIRPS and does not explicitly represent crack-flow processes
Gedaref station rainfall	Monthly, April–November	1982–2020	Station-based evaluation of CHIRPS rainfall	Point record with no information on daily rainfall sequences
Sorghum statistics	Annual	1982–2020	Administrative crop-response indicator	Influenced by management, reporting practices, and structural change
Sesame statistics	Annual	1982–2020	Administrative crop-response indicator	Reported yield disagreed with production- and area-derived yield in six years

2.3 Station-based evaluation of CHIRPS rainfall

Daily CHIRPS rainfall was aggregated to monthly totals for April–November, corresponding to the months available in the station archive. Agreement between CHIRPS and station rainfall was examined at seasonal and monthly scales using Pearson correlation, mean bias, root mean square error (RMSE), Nash–Sutcliffe efficiency (NSE), and Kling–Gupta efficiency (KGE), and Kling–Gupta efficiency (Nash and Sutcliffe, 1970; Legates and McCabe, 1999; Gupta et al., 2009; Kling et al., 2012).

The pooled monthly correlation may partly reflect the common seasonal cycle, with low rainfall near the beginning and end of the season and higher rainfall during July and August in both datasets. A second correlation was therefore calculated after subtracting the long-term mean of each calendar month from the corresponding monthly observations.

$$\mathrm{Bias} = \frac{1}{n}\sum_{i=1}^{n}\left(P_{\mathrm{CHIRPS,i}} - P_{\mathrm{station,i}}\right) \quad (1)$$

$$\mathrm{RMSE} = \sqrt{\frac{1}{n}\sum_{i=1}^{n}\left(P_{\mathrm{CHIRPS,i}} - P_{\mathrm{station,i}}\right)^2} \quad (2)$$

where n is the number of paired observations, PCHIRPS,i is CHIRPS rainfall, and Pstation,i is station rainfall for observation i.

The paired monthly CHIRPS and station rainfall series used for this evaluation are provided in Supplementary Table S16.

2.4 Daily rainfall indicators

Rainfall indicators were calculated to describe the main within-season wetting and drying conditions that cannot be seen from seasonal rainfall totals alone. Indicators were calculated for the April–November season and, where relevant, for the main June–September rainy period. A dry day was defined as a day receiving less than 1 mm of rainfall, and a wet day as a day receiving at least 1 mm. Rx1day and Rx5day were calculated as the highest single-day and the highest consecutive five-day April–November rainfall totals, following the ETCCDI definitions (Zhang et al., 2011). Rx5day is not the same as the top-five rainfall share: Rx5day requires the five days to be consecutive, while the top-five share sums the five largest daily totals wherever they occur in the season.

Rainfall onset was defined as the first date on or after 1 May when the accumulated rainfall over three consecutive days reached at least 20 mm. This definition used only the rainfall accumulated during the three-day period and did not include a condition based on rainfall during the following month. Two alternative definitions—15 mm over three days and 25 mm over five days—were evaluated in the sensitivity analysis (Stern et al., 1981; Ati et al., 2002; Marteau et al., 2011).

For year y, maximum consecutive dry days during June–September were calculated as:

$$\mathrm{CDD_y} = \max\left[\text{number of consecutive days for which } P_{y,t} < 1\ \mathrm{mm}\right] \quad (3)$$

Rainfall onset was calculated as:

$$\mathrm{Onset_y} = \min\left\{t \geq 1\ \mathrm{May}: \sum_{j=0}^{2} P_{y,t+j} \geq 20\ \mathrm{mm}\right\} \quad (4)$$

The share of seasonal rainfall received during the five wettest days was calculated as:

$$\mathrm{Top5Share_y} = 100 \times \frac{\sum_{k=1}^{5} P_{y,(k)}}{P_{\mathrm{season},y}} \quad (5)$$

where $P_{y,t}$ is daily rainfall on day t of year y, $P_{y,(k)}$ is the kth largest daily rainfall total in that year, and $P_{season,y}$ is total April–November rainfall.

Top-five rainfall share describes the concentration of rainfall among the largest daily events within a season. It is different from the precipitation concentration index, which measures how rainfall is distributed among calendar months (Oliver, 1980).

2.5 FLDAS soil-moisture variables

The FLDAS dataset provided monthly soil-moisture estimates for the 0–10, 10–40, 40–100, and 100–200 cm model layers. The primary response variable was the April–November mean of the 0–10 cm layer. This layer was selected because it responds most directly to rainfall and drying and was therefore the most relevant FLDAS layer for examining regional surface-drying exposure.

Thickness-weighted averages for the 0–100 and 0–200 cm profiles were calculated as secondary descriptors. These profile averages were used to compare the surface layer with deeper modelled storage, but they were not treated as field measurements or as direct estimates of crop root-zone water availability. The Noah model also does not explicitly represent the opening, connectivity, and closure of cracks in swelling clay soils (Bronswijk, 1988; Wilding and Tessier, 1988; Blokhuis, 1993; Hillel, 1998).

The 0–100 cm profile average was calculated as (10SM0–10 + 30SM10–40 + 60SM40–100)/100, and the 0–200 cm profile average as (10SM0–10 + 30SM10–40 + 60SM40–100 + 100SM100–200)/200.

The standardized surface soil-moisture anomaly (SSMA) was calculated as:

$$\mathrm{SSMA_y} = \frac{\mathrm{SM_y} - \overline{\mathrm{SM}}_{1982-2020}}{\mathrm{SD}(\mathrm{SM}_{1982-2020})} \quad (6)$$

where SM_y is the April–November mean surface soil moisture for year y.

2.6 Crop records and quality control

Sorghum yield was recalculated by dividing total production by productive area. The harvested-area ratio was calculated as the percentage of planted area reported as producive. The 1986 record had a harvested-area ratio of 100%. It was retained in the main analysis, and the analysis was repeated without it to assess its influence.

Sesame yield was calculated from annual production and productive area for all years. In 2014, 2015, and 2017–2020, the reported yield differed by more than 10% from the value obtained from production and productive area. The derived series was used in the main analysis to maintain a consistent calculation method across all years. A sensitivity analysis was also conducted after excluding the six inconsistent years.

Sorghum production was recorded in sacks and sesame production in qintars, while planted and productive areas were recorded in feddans. One sack of sorghum was taken as 90 kg, one qintar of sesame as 45 kg, and one feddan as 4200 m². Production was therefore converted to kilograms and area to hectares before analysis, and derived yields were expressed as kg ha^{-1} for both crops. One sack feddan^{-1} corresponds to 214.3 kg ha^{-1} for sorghum, and one qintar feddan^{-1} to 107.1 kg ha^{-1} for sesame.

The annual sesame records did not contain year-specific information on input use, access to finance, pest and disease incidence, labour availability, harvesting method, post-harvest losses, or marketing conditions. These factors could therefore not be included as covariates in the analysis.

The derived crop variables were calculated as:

$$\text{Derived yield}_\mathrm{y} = \frac{\text{Production}_\mathrm{y}}{\text{Productive area}_\mathrm{y}} \quad (7)$$

$$\text{Harvested-area ratio}_\mathrm{y} = 100 \times \frac{\text{Productive area}_\mathrm{y}}{\text{Planted area}_\mathrm{y}} \quad (8)$$

Long-term changes in technology, cultivated area, reporting, and management can produce trends in crop statistics that are unrelated to annual rainfall conditions. Each crop-response variable was therefore detrended using a Theil–Sen regression, and the residuals were standardised before the correlation analyses.

The sorghum harvested-area ratio was examined for an abrupt structural change using Pettitt's non-parametric change-point test. Where a significant change point was detected, associations with seasonal rainfall and DRSRI were examined separately for the periods before and after the identified break (Pettitt, 1979).

2.7 Construction of DRSRI

The Daily Rainfall-Structure Risk Index was constructed from four rainfall variables chosen to represent the main forms of within-season rainfall stress in rainfed lands:

1. April–November rainfall deficit;
2. maximum June–September consecutive dry days;
3. onset delay; and

4. the share of seasonal rainfall received during the five wettest days.

Seasonal rainfall deficit represented low seasonal water supply. Maximum CDD represented the length of the longest dry interruption during the main rainy period. Onset delay represented late seasonal wetting, and top-five rainfall share represented rainfall concentration in a small number of events. Together, these variables described the rainfall conditions most likely to increase surface-drying exposure at the regional scale.

Seasonal rainfall deficit was defined as the negative standardised value of April–November rainfall, so lower rainfall produced a higher risk value. Onset delay was calculated from the standardised day of year of rainfall onset. CDD and top-five rainfall share were standardised without reversing their direction because larger values represented greater risk.

The four standardised variables were examined using pairwise correlations, variance inflation factors, the Kaiser–Meyer–Olkin measure, Bartlett's test, the scree criterion, and parallel analysis. Coefficient stability was evaluated using 5,000 bootstrap samples drawn by resampling years with replacement (Bartlett, 1954; Horn, 1965; Cattell, 1966; Kaiser, 1974; O'Brien, 2007).

For each bootstrap sample, the sign of the retained PC1 solution was aligned with the positive-risk direction of the full-sample solution before the coefficient confidence intervals were calculated.

The first principal component was retained as the common rainfall-structure dimension. Its score was calculated from the eigenvector coefficients of the standardized input matrix, following standard PCA procedures (Jolliffe, 2002; Abdi and Williams, 2010; Jolliffe and Cadima, 2016). The four input variables were standardized using the population standard deviation, and the raw PC1 score was then rescaled to unit sample variance across the 39 years:

$$\mathrm{DRSRI_z} = 0.334\mathrm{Z_{rainfall_deficit}} + 0.320\mathrm{Z_{CDD}} + 0.293\mathrm{Z_{onset}} + 0.321\mathrm{Z_{concentration}} \quad (9)$$

The coefficients shown in Equation 9 are standardized PCA score coefficients obtained from the unrounded eigenvector after rescaling to unit sample variance. Dividing each eigenvector element by the square root of the eigenvalue alone would give values about 1.3% larger, because the rescaling carries the additional factor √(n/(n − 1)) with n = 39. The coefficients are not proportional weights and are not expected to sum to one. Their normalised relative contributions were approximately 26.3%, 25.2%, 23.1%, and 25.3%, respectively.

2.8 Temporal evaluation and model comparison

Temporal transferability was examined using two fixed holdout tests. First, the standardisation parameters and PCA coefficients were estimated from 1982–2001 and applied to 2002–2020. The analysis was then reversed, using 2002–2020 for construction and 1982–2001 for evaluation. Each holdout compared three predictors: seasonal rainfall, the four rainfall variables entered separately, and DRSRI.

All predictive models were fitted using ordinary least-squares linear regression with an intercept. In each temporal holdout and rolling-origin step, standardisation parameters, PCA coefficients, and regression coefficients were estimated exclusively from the available training period and were then applied unchanged to the corresponding validation year or holdout period.

Predictive performance was also evaluated using rolling-origin validation. Models were initially fitted using 1982–1996 and were refitted after each additional year became available. This produced one out-of-sample prediction for every year from 1997 to 2020, using only information from preceding years.

Four models were compared:

i. seasonal rainfall alone;
ii. the four daily rainfall variables;
iii. DRSRI alone; and
iv. seasonal rainfall together with DRSRI.

Performance was summarised using RMSE, mean absolute error, cross-validated R^2, and the correlation between observed and predicted surface soil-moisture anomalies. Confidence intervals for the RMSE of each model were obtained from 20,000 bootstrap resamples of the annual prediction errors, and the difference in RMSE between the daily-variable model and the seasonal-rainfall model was evaluated using 20,000 paired bootstrap resamples of the same errors. Statistical evidence of a difference in predictive error was assessed from the 95% paired-bootstrap confidence interval for ΔRMSE; an interval excluding zero indicated a difference between the models (Stone, 1974; Efron and Tibshirani, 1993; Hastie et al., 2009).

$$R^2_{CV} = 1 - \frac{\sum_{i=1}^{n}\left(Y_i - \hat{Y}_i\right)^2}{\sum_{i=1}^{n}\left(Y_i - \overline{Y}\right)^2} \quad (10)$$

where Y_i is the observed anomaly, $\hat{Y}_i$ is the corresponding out-of-sample prediction, $\bar{Y}$ is the mean observed anomaly across the evaluation years, and n is the number of out-of-sample predictions.

2.9 Agricultural response, compound rainfall-risk years, and trend analysis

Pearson correlations were used for the six primary predictor–response tests, and their p-values were adjusted using the Benjamini–Hochberg procedure. Spearman correlations were reported as sensitivity analyses and were not included in the primary false-discovery-rate family (Benjamini and Hochberg, 1995).

Compound rainfall-risk conditions were defined separately for each year. One point was assigned for each of the following:

- seasonal rainfall at or below the 25th percentile;
- onset date at or above the 75th percentile;
- maximum CDD at or above the 75th percentile; and
- top-five rainfall concentration at or above the 75th percentile.

Years satisfying at least three of the four conditions were classified as compound-risk years. Differences in modelled surface soil moisture and crop-response variables between compound-risk and other years were tested using 20,000 random permutations of the year labels. False-discovery-rate correction was applied across the four response variables. Two-sided permutation p-values were calculated as $(b + 1)/(B + 1)$, where b was the number of permuted absolute mean differences equal to or greater than the observed absolute difference and B was the number of permutations.

The robustness of the compound-event classification was examined using P20/P80, P25/P75, and P30/P70 thresholds and rules requiring two, three, or four simultaneous conditions, each evaluated with 5,000 permutations (Zscheischler et al., 2018, 2020).

Two variants of the index were also examined: an equal-weight average of the four standardized variables, and a version in which the dry-day threshold used for consecutive dry days was raised from 1 mm to 2 mm.

Trend-free prewhitening was applied before Mann–Kendall trend testing. Sen's slope was used to estimate the magnitude of change, and false-discovery-rate correction was applied across the family of eleven trend tests (Mann, 1945; Sen, 1968; Kendall, 1975; Hamed and Rao, 1998; Yue et al., 2002; Yue and Wang, 2004).

Effect sizes, confidence intervals, and consistency across sensitivity analyses were considered together when interpreting the statistical results (Wilks, 2011). Detailed temporal-holdout, trend, and sensitivity results are provided in the supplementary file. All analyses were conducted in Python 3.12.1 using the pandas (v2.2.0), NumPy (v1.26.4), SciPy (v1.12.0), scikit-learn (v1.4.2), and Matplotlib (v3.5.2) libraries.

3. Results

3.1 Data completeness and CHIRPS evaluation

The dataset included 14,245 daily CHIRPS observations, 468 monthly FLDAS observations, and 39 annual records for each crop. For April–November seasonal rainfall, CHIRPS and station records had a correlation of $r = 0.625$ ($R^2 = 0.391$). Mean bias was −77.5 mm, RMSE was 130.0 mm, NSE was 0.055, and KGE was 0.460.

For pooled April–November monthly totals, the correlation was $r = 0.862$ ($R^2 = 0.743$). Mean monthly bias was −9.7 mm, RMSE was 45.8 mm, NSE was 0.716, and KGE was 0.680. After removal of the long-term mean for each calendar month, the correlation between monthly anomalies was $r = 0.542$ ($R^2 = 0.294$).

The CHIRPS evaluation statistics are summarised in Table 2.

Table 2. CHIRPS evaluation against the Gedaref station archive, 1982–2020.

Scale	n	r	R^2	Bias	RMSE	NSE	KGE
Seasonal April–November	39	0.625	0.391	−77.5 mm	130.0 mm	0.055	0.460
Pooled monthly April–November	312	0.862	0.743	−9.7 mm	45.8 mm	0.716	0.680
Month-demeaned anomalies	312	0.542	0.294	—	—	—	—

Bias was calculated as CHIRPS minus station rainfall; negative values indicate CHIRPS underestimation.

3.2 Rainfall structure and modelled surface drying

Mean April–November rainfall was 525.0 mm, with a standard deviation of 85.8 mm and a range from 324.0 to 701.6 mm. The mean number of wet days receiving at least 1 mm was 105.2 days per season, ranging from 75 to 130 days. The range in wet-day counts points to clear year-to-year differences that were not captured by the seasonal total alone. The wet-day occurrence pattern is shown in Figure 3.

Maximum June–September CDD averaged 6.1 days and ranged from 2 to 13 days. Mean rainfall onset occurred on day 179.3 of the year, with onset dates ranging from day 135 to day 240. Mean Rx1day was 18.3 mm, while mean Rx5day was 50.5 mm. The five wettest days contributed an average of 14.2% of April–November rainfall, with annual values ranging from 10.2% to 21.0%. Together, these indicators describe marked year-to-year variation in rainfall timing, continuity, and concentration, even at the state-average scale.

Mean April–November FLDAS surface soil moisture was 0.248 $m^3\ m^{-3}$ and ranged from 0.212 to 0.286 $m^3\ m^{-3}$. The standardised surface soil-moisture anomaly ranged from −2.229 to 2.398. Monthly surface soil moisture increased during the rainy season, reached its highest mean values in August and September, and then declined during October and November. The deeper FLDAS layers showed smaller monthly variation than the 0–10 cm layer, as shown in Figure 4.

Accordingly, the surface layer was retained as the main modelled response for examining seasonal wetting and surface-drying exposure. Descriptive statistics of the principal rainfall and surface-moisture indicators are presented in Table 3.

Table 3. Descriptive statistics of the principal rainfall and modelled surface-moisture indicators.

Indicator	Mean	SD	Minimum	Maximum
April–November rainfall (mm)	525.0	85.8	324.0	701.6
Wet days ≥1 mm (days)	105.2	12.2	75.0	130.0
Maximum CDD, June–September (days)	6.1	2.8	2.0	13.0
Onset day of year	179.3	22.5	135.0	240.0
Rx1day (mm)	18.3	3.9	11.3	27.4
Rx5day (mm)	50.5	9.1	33.6	71.0
Top-five wet-day share (%)	14.2	2.3	10.2	21.0
Surface soil moisture, April–November ($m^3\ m^{-3}$)	0.248	0.016	0.212	0.286
Surface SSMA	0.000	1.000	−2.229	2.398

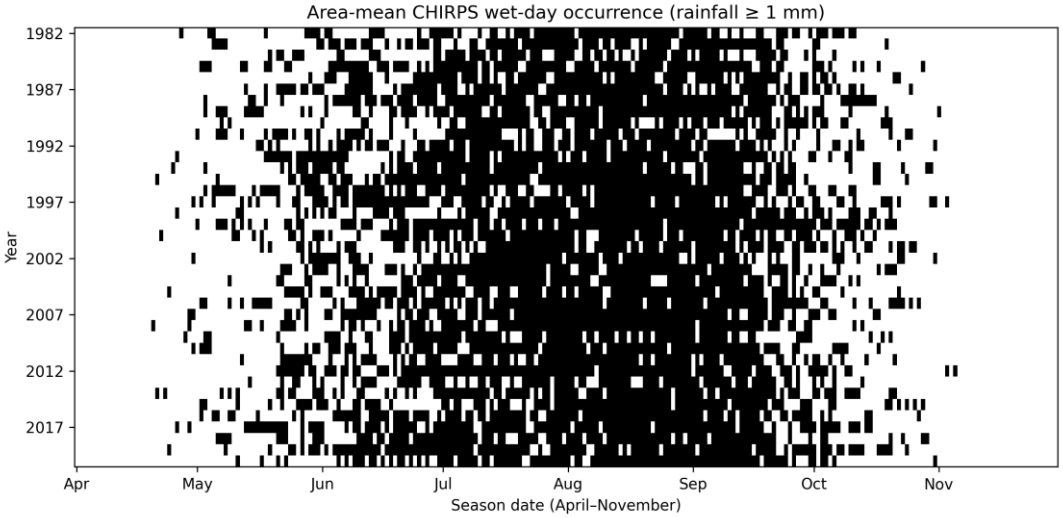


Figure 3. Area-mean CHIRPS wet-day occurrence during April–November, 1982–2020. Black cells indicate days when the state-wide mean rainfall was at least 1 mm.

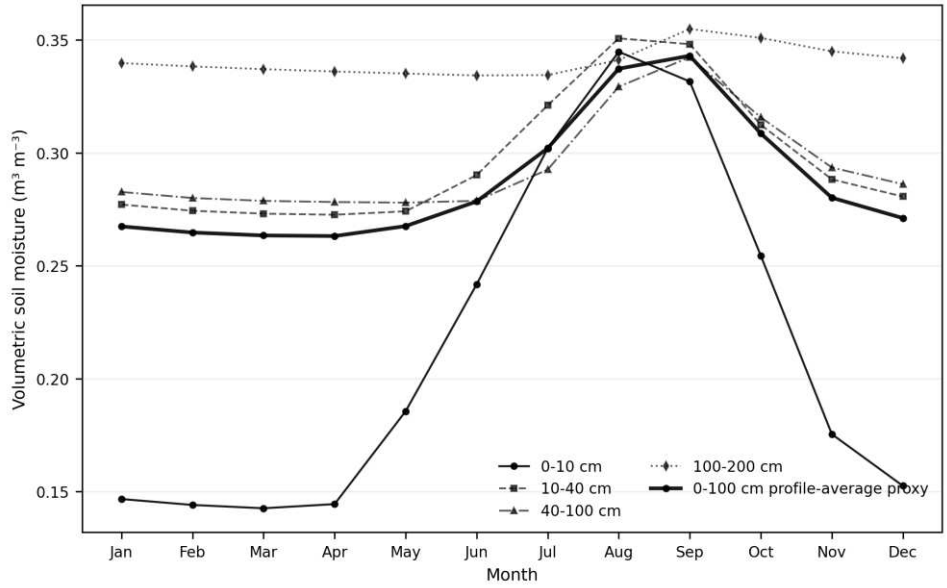


Figure 4. Mean monthly FLDAS soil moisture by model layer and for the 0–100 cm profile-average proxy, 1982–2020. The 0–10 cm layer was used as the main modelled surface-drying response layer.

3.3 DRSRI diagnostics and coefficients

The Kaiser–Meyer–Olkin value for the four-variable matrix was 0.762. Bartlett's test was significant ($\chi^2 = 39.07$, df = 6, $p < 0.001$). Variance inflation factors ranged from 1.378 to 1.760.

Parallel analysis retained one principal component. The first observed eigenvalue was 2.418, above the corresponding threshold obtained from randomly generated data, while the second observed eigenvalue was 0.625 and fell below its threshold. PC1 explained 60.4% of the standardized variance. Eigenvector coefficients ranged from 0.462 for onset delay to 0.526 for seasonal rainfall deficit. Because the sign of each bootstrap solution was aligned with the positive-risk direction before the intervals were calculated, the intervals describe the stability of the relative coefficient magnitudes rather than the statistical significance of individual coefficients. On this basis, the four coefficients remained of comparable size across resamples, and none collapsed towards zero. The PCA coefficients and diagnostics are presented in Table 4 and Figure 5, while the annual DRSRI series is shown in Figure 6.

Table 4. Rainfall-only PCA coefficients and diagnostics used to construct DRSRI.

Risk component	PC1 coefficient	Standardised equation coefficient	Bootstrap 95% CI for PC1 coefficient	VIF
Seasonal rainfall deficit	0.526	0.334	0.469–0.608	1.760
Maximum CDD, June–September	0.504	0.320	0.379–0.611	1.584
Onset delay	0.462	0.293	0.230–0.533	1.378
Top-five rainfall concentration	0.506	0.321	0.366–0.584	1.594

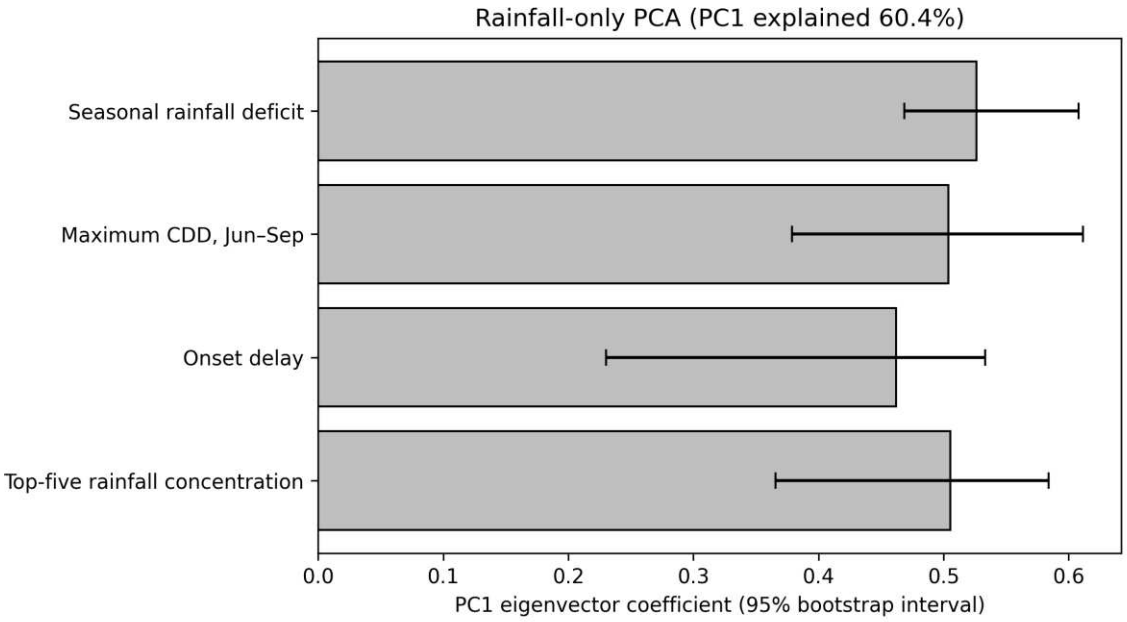


Figure 5. Rainfall-only PCA coefficients and their 95% bootstrap intervals.

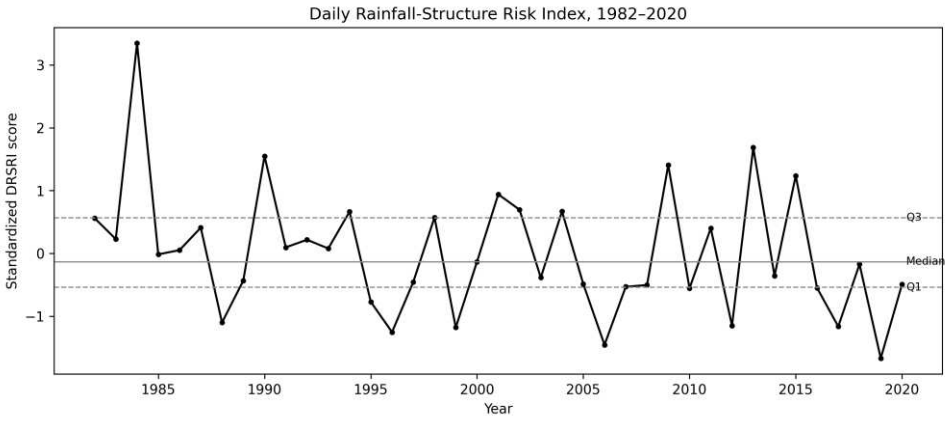


Figure 6. Annual standardized DRSRI values during 1982–2020. Horizontal reference lines indicate the first quartile, median, and third quartile.

3.4 Rainfall-structure risk and modelled surface drying

Across the full 1982–2020 record, higher DRSRI values were associated with lower FLDAS surface SSMA ($r = -0.776$, $p < 0.001$). Years with less favourable rainfall structure therefore tended to show stronger modelled surface-drying exposure. When the index and model coefficients were estimated using 1982–2001 and evaluated during 2002–2020, the observed–predicted surface SSMA correlations were 0.808 for the seasonal-rainfall model, 0.841 for the four-variable daily rainfall

model, and 0.768 for the DRSRI model. Both seasonal rainfall and daily rainfall structure retained information about modelled surface moisture in the later period.

When the construction and evaluation periods were reversed, the corresponding observed–predicted correlations were 0.946 for seasonal rainfall, 0.955 for the four daily rainfall variables, and 0.807 for DRSRI. The relationship was therefore present in both temporal directions, although the four rainfall variables retained more information than the single index.

Associations with the 0–100 cm profile-average proxy were lower than those obtained for the 0–10 cm surface layer. In the 1982–2001 holdout the observed–predicted correlations for the 0–100 cm proxy were 0.330, 0.291, and 0.238 for the three models, and in the reversed holdout they were 0.711, 0.580, and 0.513. This supports the choice of the surface layer as the main response variable for rainfall-related drying. The full temporal-holdout results for both soil-moisture variables are presented in Supplementary Table S6.

3.5 Rolling-origin model comparison

Rolling-origin evaluation used 1982–1996 as the initial training period and generated 24 sequential predictions for 1997–2020. This test examined whether rainfall variables estimated from earlier years could track later variation in modelled surface soil moisture.

For surface SSMA, the seasonal-rainfall model had an RMSE of 0.554 standardised units and an MAE of 0.471. The four-variable daily rainfall model had an RMSE of 0.544 and an MAE of 0.452. The difference in RMSE between the two models was small, at −0.011 standardized units, and the 95% bootstrap confidence interval included zero (−0.080 to 0.060; p = 0.739).

The DRSRI model had an RMSE of 0.681 and an MAE of 0.566. The combined seasonal-rainfall and DRSRI model had an RMSE of 0.549 and an MAE of 0.474. Cross-validated R^2 ranged from 0.485 for the DRSRI model to 0.671 for the four-variable daily rainfall model. DRSRI served as a compact risk summary, but the separate rainfall variables provided the strongest rolling-origin performance. Rolling-origin performance is summarised in Table 5 and Figure 7.

Table 5. Rolling-origin benchmark for April–November FLDAS surface soil-moisture anomaly.

Model	n	RMSE	Bootstrap 95% CI	MAE	CV R^2	Observed–predicted r
Seasonal rainfall	24	0.554	0.424–0.683	0.471	0.658	0.814
Daily rainfall structure	24	0.544	0.405–0.675	0.452	0.671	0.822
DRSRI	24	0.681	0.513–0.840	0.566	0.485	0.711
Seasonal rainfall + DRSRI	24	0.549	0.433–0.661	0.474	0.665	0.818

Note: The paired bootstrap comparison between the four-variable daily rainfall model and the seasonal-rainfall model gave ΔRMSE = −0.011 standardized units (95% CI: −0.080 to 0.060; p = 0.739). ΔRMSE was computed from unrounded RMSE values and therefore differs slightly from the difference between the rounded values shown in the table.

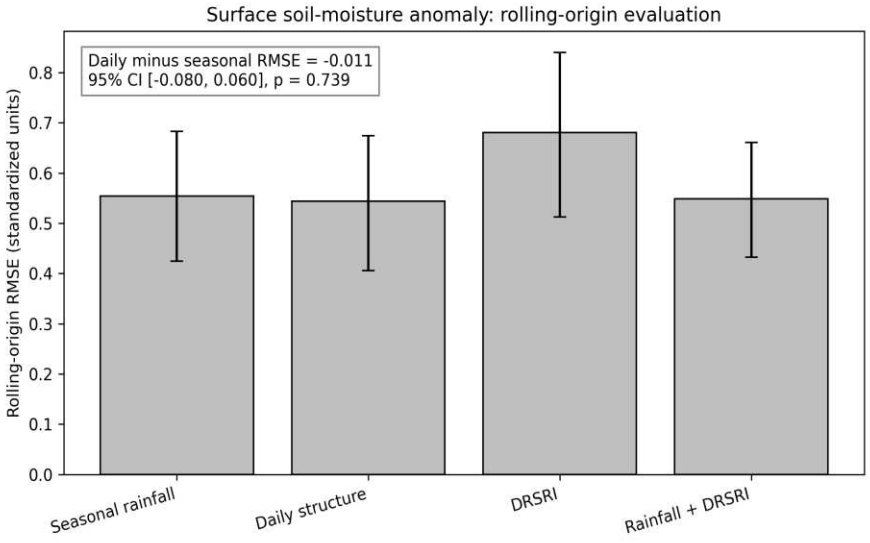


Figure 7. Rolling-origin RMSE for the surface soil-moisture models. Error bars indicate 95% bootstrap confidence intervals.

3.6 Agricultural response associations

After Theil–Sen detrending, the clearest agricultural response was found for the sorghum harvested-area ratio anomaly. Seasonal rainfall was positively correlated with this response (r = 0.440, p = 0.005, FDR-adjusted p = 0.015), while DRSRI was negatively correlated with it (r = −0.448, p = 0.004, FDR-adjusted p = 0.015). Years with higher rainfall-structure risk were therefore associated with a lower proportion of planted sorghum area reported as productive.

Sorghum yield showed weaker associations than the harvested-area ratio. Seasonal rainfall was correlated with sorghum yield anomaly at r = 0.327, with an unadjusted p-value of 0.042 and an FDR-adjusted p-value of 0.084. The correlation between DRSRI and sorghum yield anomaly was r = −0.294, with p = 0.069 and an FDR-adjusted p-value of 0.085.

Sesame derived-yield anomaly showed no clear adjusted association with either rainfall measure. The correlations were r = 0.134 for seasonal rainfall and r = −0.293 for DRSRI. The corresponding FDR-adjusted p-values were 0.416 and 0.085, respectively. Primary agricultural response correlations are reported in Table 6, and their confidence intervals are shown in Figure 8.

Table 6. Primary agricultural response correlations after Theil–Sen detrending.

Predictor	Response	n	r	95% CI	p	FDR-adjusted p
Seasonal rainfall	Sorghum yield anomaly	39	0.327	0.013–0.583	0.042	0.084
Seasonal rainfall	Sorghum harvested-area ratio anomaly	39	0.440	0.144–0.663	0.005	0.015
Seasonal rainfall	Sesame derived-yield anomaly	39	0.134	−0.190–0.431	0.416	0.416
DRSRI	Sorghum yield anomaly	39	−0.294	−0.558–0.023	0.069	0.085
DRSRI	Sorghum harvested-area ratio anomaly	39	−0.448	−0.669 to −0.155	0.004	0.015
DRSRI	Sesame derived-yield anomaly	39	−0.293	−0.557–0.025	0.071	0.085

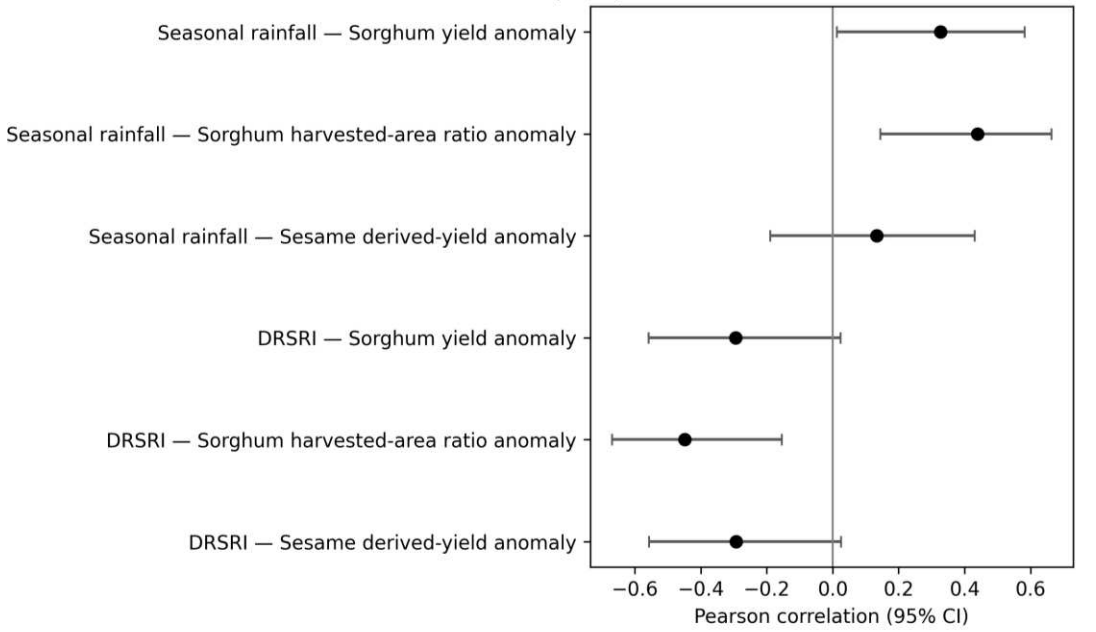


Figure 8. Pearson correlations and 95% confidence intervals between rainfall predictors and detrended agricultural response variables. FDR-adjusted p-values are reported in Table 6.

3.7 Sensitivity of agricultural response analyses

Pettitt's test identified a significant change point after 1996 in the sorghum harvested-area ratio (K = 284, p = 0.0007). The series was therefore divided into 1982–1996 and 1997–2020 for the sub-period analyses.

After excluding the 1986 sorghum record, the correlation between DRSRI and the harvested-area ratio anomaly was r = −0.451 (p = 0.004). The corresponding Spearman correlation was ρ = −0.274 (p = 0.096).

During 1982–1996, DRSRI was correlated with the sorghum harvested-area ratio anomaly at r = −0.688 (p = 0.005); during 1997–2020, the correlation was r = −0.329 (p = 0.117).

For seasonal rainfall, the corresponding correlations were r = 0.492 (p = 0.062) during 1982–1996 and r = 0.554 (p = 0.005) during 1997–2020.

After excluding the six sesame years with inconsistent reported yields, the DRSRI correlation with sesame derived-yield anomaly was r = −0.284 (p = 0.109), and the Spearman correlation was ρ = −0.334 (p = 0.058). The corresponding seasonal-rainfall correlation was r = 0.091 (p = 0.613). Sensitivity results are summarised in Table 7.

The alternative onset definitions gave similar seasonal timing. Mean onset was day 166.4 under the 15 mm over three days rule and day 178.6 under the 25 mm over five days rule, against day 179.3 for the primary rule, and the alternative series correlated with the primary series at r = 0.637 and r = 0.852. Replacing the PCA weights with equal weights left the index almost unchanged (r = 0.9997 with the primary DRSRI), and raising the dry-day threshold from 1 mm to 2 mm gave an index correlated with the primary DRSRI at r = 0.979. Under both variants the correlation with surface soil moisture (r = −0.766 and r = −0.782) and with the sorghum harvested-area ratio anomaly (r = −0.447 and r = −0.452) stayed close to the primary values. Full sensitivity results are given in Supplementary Tables S13 and S15.

The negative CHIRPS bias against the station record may partly reflect the difference in spatial support, because the station represents a single point in Gedaref town whereas the CHIRPS series is a state-wide mean that includes drier northern localities.

Table 7. Sensitivity of agricultural response associations to data-quality screening and the 1996 structural break.

Analysis	Subset	n	Pearson r	Pearson p	Spearman ρ	Spearman p
DRSRI vs. sorghum harvested-area ratio anomaly	Excluding 1986	38	−0.451	0.004	−0.274	0.096
DRSRI vs. sesame derived-yield anomaly	Excluding six inconsistent years	33	−0.284	0.109	−0.334	0.058
Seasonal rainfall vs. sesame derived-yield anomaly	Excluding six inconsistent years	33	0.091	0.613	0.014	0.938
DRSRI vs. sorghum harvested-area ratio anomaly	1982–1996	15	−0.688	0.005	−0.579	0.024
Seasonal rainfall vs. sorghum harvested-area ratio anomaly	1982–1996	15	0.492	0.062	0.396	0.143
DRSRI vs. sorghum harvested-area ratio anomaly	1997–2020	24	−0.329	0.117	−0.237	0.266
Seasonal rainfall vs. sorghum harvested-area ratio anomaly	1997–2020	24	0.554	0.005	0.410	0.046

Note: Crop-response variables were detrended using Theil–Sen regression. The first sensitivity analysis excluded the 1986 sorghum record, for which the harvested-area ratio was 100%. The sesame sensitivity analysis excluded 2014, 2015, and 2017–2020 because reported yield differed by more than 10% from yield calculated from production and productive area.

3.8 Compound rainfall-risk years and surface-drying response

Eight years met at least three of the four compound rainfall-risk conditions: 1984, 1990, 1998, 2001, 2004, 2009, 2013, and 2015.

Mean surface SSMA was −0.970 during compound-risk years and 0.250 during the remaining years, giving a difference of −1.220 standardised units. The two-sided permutation p-value was 0.0012, and the FDR-adjusted p-value was 0.0025. Compound-risk years therefore showed substantially lower modelled surface moisture than other years.

Mean sorghum harvested-area ratio anomaly was −0.956 during compound-risk years and 0.247 during other years. The difference was −1.203 standardised units, with a two-sided permutation p-value of 0.0009 and an FDR-adjusted p-value of 0.0025. The proportion of planted sorghum area reported as productive was lower in years when several rainfall-risk conditions occurred together.

The differences were −0.591 standardised units for sorghum yield anomaly and −0.715 standardised units for sesame derived-yield anomaly. Their FDR-adjusted p-values were 0.1368 and 0.0974, respectively, indicating weaker evidence for yield responses than for surface moisture and sorghum harvested-area ratio.

Across the alternative P20/P80, P25/P75, and P30/P70 definitions, the mean differences in surface SSMA and sorghum harvested-area ratio anomaly remained negative. The number of years classified as compound-risk years varied among the alternative definitions. The direction of the main response was stable, although the exact set of compound-risk years depended on the chosen threshold. Compound-year responses are summarised in Table 8 and Figure 9.

Table 8. Modelled surface-moisture and agricultural responses during the primary compound-risk years.

Response	Compound-risk years	Other years	Difference	Permutation p	FDR-adjusted p
Surface soil-moisture anomaly	−0.970	0.250	−1.220	0.0012	0.0025
Sorghum harvested-area ratio anomaly	−0.956	0.247	−1.203	0.0009	0.0025
Sorghum yield anomaly	−0.470	0.121	−0.591	0.1368	0.1368
Sesame derived-yield anomaly	−0.568	0.147	−0.715	0.0730	0.0974

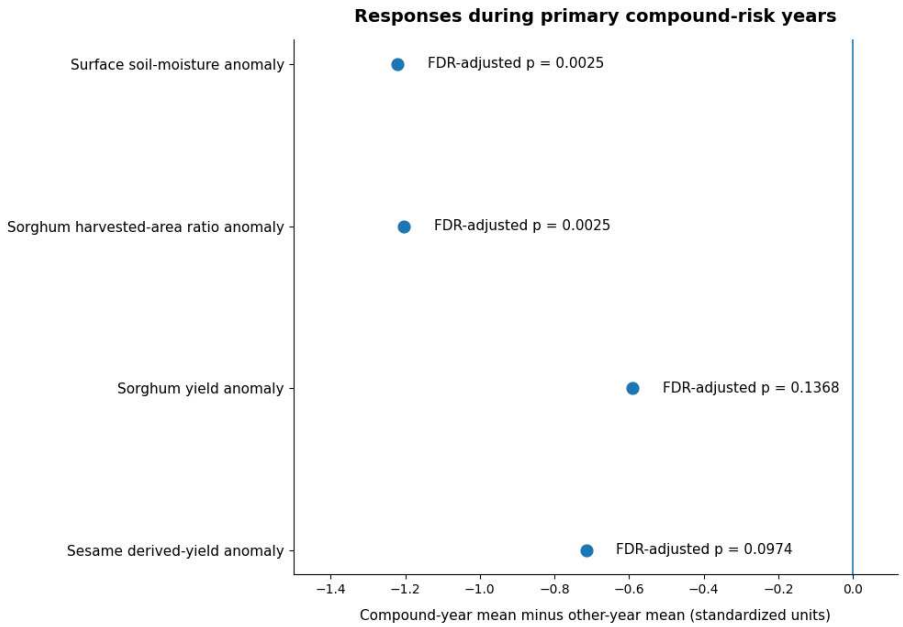


Figure 9. Differences in mean standardized modelled surface-moisture and agricultural responses between compound-risk and other years. FDR-adjusted p-values are shown beside the points.

3.9 Long-term trends

After trend-free prewhitening and false-discovery-rate correction across the eleven trend tests, none of the rainfall indicators changed significantly during 1982–2020. April–November rainfall rose by 26.9 mm per decade ($\tau = 0.195$, FDR-adjusted $p = 0.204$), wet days rose by 3.2 days per decade ($\tau = 0.164$, FDR-adjusted $p = 0.204$), maximum June–September CDD fell by 0.65 days per decade ($\tau = -0.172$, FDR-adjusted $p = 0.204$), onset shifted by −1.3 days per decade ($\tau = -0.067$, FDR-adjusted $p = 0.555$), top-five rainfall concentration fell by 0.50 percentage points per decade ($\tau = -0.164$, FDR-adjusted $p = 0.204$), and DRSRI fell by 0.22 standardized units per decade ($\tau = -0.166$, FDR-adjusted $p = 0.204$). Two response variables did change significantly: the FLDAS 0–100 cm soil-moisture anomaly rose by 0.38 standardized units per decade ($\tau = 0.428$, FDR-adjusted $p = 0.001$), and the sorghum harvested-area ratio fell by 9.19 percentage points per decade ($\tau = -0.420$, FDR-adjusted $p = 0.001$). The surface soil-moisture anomaly rose by 0.31 standardized units per decade, but this was not significant after correction ($\tau = 0.243$, FDR-adjusted $p = 0.116$). The decline in the sorghum harvested-area ratio supports the decision to detrend the crop-response variables before the correlation analyses. Full trend statistics are given in Supplementary Table S14.

4. Discussion

4.1 Rainfall structure and surface-drying risk in rainfed lands

Seasonal rainfall totals gave only a partial description of rainfall risk in Gedaref. The annual amount of rainfall remained important, but it did not explain how rainfall was distributed through the growing season. Some years had later onset, longer dry intervals during the main rainy period, or a larger share of rainfall delivered by a few wet days. These features matter in rainfall-dependent farming because soil and crops respond to the sequence of wetting and drying, not only to the seasonal total.

In degradation-prone rainfed lands, these differences can affect the surface soil even in seasons that are not extremely dry. Late onset shortens the period available for crop growth. A long dry spell can interrupt establishment or early growth. Rainfall concentrated in a few events may leave long dry intervals between storms. For this reason, rainfall structure gives a clearer view of seasonal exposure than rainfall totals alone.

In the rolling-origin test, the four daily rainfall variables did not clearly improve prediction compared with seasonal rainfall alone. Their RMSE was slightly lower, but the difference was small and the confidence interval included zero. Seasonal rainfall therefore remained a strong summary predictor of modelled surface moisture. The daily variables were still useful because they identified the type of seasonal problem: late onset, a long dry spell, or rainfall concentrated in a few events.

4.2 Modelled surface drying and the role of the upper soil layer

Higher DRSRI values were associated with lower FLDAS surface soil-moisture anomalies over the full record and in both temporal holdout tests. Years with lower rainfall, later onset, longer June–September dry spells, and higher rainfall concentration tended to be years with lower modelled moisture in the 0–10 cm layer. This agrees with the expected behaviour of the upper soil layer, which wets quickly after rainfall and dries faster than deeper layers. The upper soil layer receives rainfall first and loses water quickly through evaporation, runoff processes, and redistribution to deeper layers.

The relationship with the 0–100 cm profile-average proxy was weaker than the relationship with the 0–10 cm layer. This pattern is consistent with the slower response of deeper soil layers. Deeper layers respond more slowly and integrate water movement over longer periods. They also smooth short dry and wet episodes that are visible near the surface. Accordingly, the surface layer was the more suitable response variable for examining seasonal rainfall structure and surface-drying exposure.

The FLDAS result should be read with this dependency in mind. Because CHIRPS rainfall is part of the forcing used by FLDAS, the comparison is not an independent validation. It shows that the rainfall indicators and the modelled surface response changed in the same direction. At the regional scale, the comparison is informative, but it cannot replace direct soil-moisture observations or describe root-zone water availability at plot level.

Cracking clay soils add another layer of uncertainty. The Noah land-surface model does not explicitly represent crack opening, preferential flow, or crack closure (Bronswijk, 1988; Wilding and Tessier, 1988; Hillel, 1998). The result is best read as a regional modelled signal of surface drying, not as a direct measurement of soil-water behaviour within individual Vertisol fields.

4.3 The meaning and use of DRSRI

DRSRI was designed as a compact annual summary of rainfall-structure risk. The four components had similar PCA coefficients, and the PCA-based index was almost identical to an equal-weight average of the four standardised variables ($r = 0.9997$). No single variable dominated the index. Rainfall deficit, dry-spell length, onset delay, and rainfall concentration each contributed to the final score.

The four components contributed in similar proportions, so the index is best used as an annual screening measure. It does not point to one single cause of risk. Instead, it brings together rainfall deficit, onset delay, dry-spell length, and rainfall concentration. The index is useful for comparing years, while the individual components remain necessary for identifying the main rainfall constraint in each season. At the same time, the index should not replace the individual indicators. The four rainfall variables performed better than DRSRI in the rolling-origin evaluation. The separate variables carried details that were partly reduced when they were combined into one score. DRSRI is therefore best used as a screening and communication tool. Once a high-risk year is identified, the component indicators are needed to understand whether the main issue was low seasonal rainfall, delayed onset, a long dry spell, or rainfall concentration.

The equation provided allows the index to be reproduced for the 1982–2020 period. Applying it outside this period or in another region would require recalculation of the standardisation parameters and local evaluation against rainfall, soil-moisture, and land-use conditions (Mishra and Singh, 2010; Zargar et al., 2011). This is particularly important because the meaning of a “late” onset or a “long” dry spell depends on the local rainfall regime and crop calendar.

4.4 Agricultural response and the 1996 structural change

The clearest agricultural response was found for the sorghum harvested-area ratio rather than yield. Yield is calculated from land that was reported as productive. It may not fully capture years in which crops failed to establish, were abandoned, or did not reach harvest. The harvested-area ratio is closer to this wider exposure. It describes the proportion of planted area that remained productive in the administrative records.

Seasonal rainfall was positively associated with the detrended sorghum harvested-area ratio, while DRSRI was negatively associated with it. Years with more favourable rainfall conditions tended to have a larger proportion of planted sorghum area reported as productive. Years with higher rainfall-structure risk tended to have a smaller proportion. The harvested-area ratio is an administrative indicator, so the relationship should be read as an association with broad crop exposure rather than a direct agronomic response to rainfall alone.

The relationship changed over time. Pettitt’s test identified a structural change after 1996, and the DRSRI relationship with the harvested-area ratio was stronger during 1982–1996 than during 1997–2020. This shift limits a simple interpretation of the full-period correlation. The weaker relationship after 1996 suggests that other factors became more important, or that the meaning of the harvested-area ratio changed through time. These factors may include changes in cultivated area, expansion into less suitable land, reporting procedures, access to inputs, labour availability, or production systems. The available annual data do not allow these influences to be separated.

The trend analysis showed the same picture from a different angle: the sorghum harvested-area ratio declined by about nine percentage points per decade across the record, while none of the rainfall indicators changed significantly. The long-

term decline in reported productive area therefore reflects factors other than a drying rainfall regime, which is why the crop series were detrended before the correlations were examined.

Sorghum yield showed weaker relationships with rainfall and DRSRI after correction for multiple testing. This pattern is consistent with the wider influence of management and reporting factors on yield. Yield reflects the performance of harvested fields and is shaped by cultivar, sowing date, soil fertility, pest pressure, management, and input use. Without annual information on these factors, yield cannot be expected to follow rainfall structure closely every year.

The sesame results were weaker than the sorghum harvested-area response. Excluding the six years with inconsistent reported yields did not substantially change the DRSRI correlation. The weak relationship was unlikely to be explained only by those data-quality issues. Sesame production in Gedaref is affected by finance, input access, labour requirements, capsule shattering, pests and diseases, transport, and post-harvest handling (Babiker, 2010; UNIDO, 2017; Ibrahim and Muhieldeen, 2018; Abdalla, 2022; Usman et al., 2022). These factors can easily weaken the annual rainfall signal. The present results therefore do not show a stable sesame response to rainfall structure.

4.5 Compound rainfall-risk years

The compound-risk analysis brought together the main rainfall stresses into one seasonal classification. Eight years met at least three of the four adverse conditions. These years had lower modelled surface soil moisture and lower sorghum harvested-area ratio anomalies than other years. The yield differences were also negative, but they were weaker and were not significant after FDR correction.

Land and crop stress often develop from several rainfall conditions occurring together. A season may not be the driest by total rainfall, but it can still be difficult for rainfed agriculture if rainfall starts late, stops for a long period, and arrives in a few concentrated events. The compound classification was useful for identifying this type of season. The alternative thresholds changed the number of years classified as compound-risk years, but the direction of the response remained similar. Surface SSMA and sorghum harvested-area ratio anomalies were generally lower in compound-risk years. The response was therefore not tied to one exact threshold definition.

Such patterns are common in dryland farming, where rainfall stresses often combine and one stress can strengthen the effect of another (Zscheischler et al., 2018, 2020). In rainfed agricultural lands, low rainfall, delayed onset, dry spells, and rainfall concentration are not isolated problems. They interact within the season and influence the wetting and drying conditions experienced by soil and crops.

4.6 Implications for degraded-land monitoring and management

The results are mainly useful for regional monitoring. Daily rainfall indicators can show whether a season had low rainfall, late onset, a long dry spell, or rainfall concentrated in a few events. This can help identify years that need closer field checking, especially when seasonal rainfall totals alone suggest less risk than was actually experienced by the surface soil.

DRSRI provides a single annual summary of rainfall-structure risk. It is useful for comparing years, but it should not be used alone. The component variables are still needed because they show the type of rainfall problem behind the index value. A delayed onset, a long dry spell, and concentrated rainfall may require different field responses.

The framework is not meant to guide individual decisions on sowing, replanting, soil-water conservation, or restoration. Those decisions require local information on soil condition, crop stage, slope, residue cover, management, and observed soil moisture. The role of the framework is to identify seasons that may deserve closer attention and, when combined with spatial land information, to guide where field checking should be prioritized.

For monitoring land susceptible to degradation, the rainfall indicators can be combined with cropland maps, soil information, and vegetation cover. Erosion indicators and field observations can then be used to check the areas that appear most exposed. Used in this way, they can help identify rainfall-dependent farming areas where unfavourable rainfall structure may increase surface-drying exposure.

4.7 Study limitations and future work

The analysis used state-level averages. This was appropriate for a regional screening study, but it reduced local variability. Convective storms may wet one part of the state while leaving another dry. State-level averaging can therefore smooth rainfall extremes and shorten estimated dry spells compared with conditions at individual fields. It also includes land outside cropped areas and soil units other than Vertisols.

The station record was monthly. It allowed comparison of accumulated rainfall, but it could not be used to test CHIRPS onset dates, daily wet-day occurrence, or consecutive dry days. FLDAS soil moisture was also monthly and partly dependent on CHIRPS rainfall forcing. The soil-moisture analysis therefore described consistency with a land-surface model, not agreement with independent field measurements.

The trend analysis also showed a significant increase in the modelled 0–100 cm soil-moisture anomaly that was not matched by a significant trend in any rainfall indicator. Long modelled soil-moisture records can drift for reasons unrelated to rainfall, including changes in the forcing datasets and the slow adjustment of deeper model layers. The deeper FLDAS layers were therefore used only as secondary descriptors and were not interpreted as evidence of long-term wetting.

The crop records were annual administrative statistics. They did not include sowing dates, crop varieties, fertiliser use, pest damage, field location, labour availability, or management practices. The structural change in the sorghum harvested-area ratio and the inconsistencies in the sesame records also limited crop-response interpretation. These limitations are part of the reality of long-term agricultural records in data-scarce regions, and they should be considered when using the results.

Future work should calculate rainfall indicators at pixel level within mapped cropland, compare CHIRPS with daily station observations, and include independent soil-moisture data where available. Field-scale information on soil properties, crop management, establishment failure, and land condition would help determine whether rainfall-structure indicators can support local decisions. Linking DRSRI with vegetation cover, erosion risk, and repeated surface-drying patterns would also make the framework more directly useful for degraded-land monitoring.

5. Conclusions

Seasonal rainfall totals did not capture the full pattern of rainfall risk in Gedaref's rainfed agricultural lands. Onset timing, consecutive dry days, and the concentration of rainfall in a few wet days showed important differences between seasons with otherwise comparable rainfall totals. When combined with seasonal rainfall deficit, these variables produced a rainfall-only index that summarised the main forms of within-season rainfall-structure risk.

DRSRI was strongly associated with lower modelled surface soil moisture, indicating that years with unfavourable rainfall structure were also years of greater surface-drying exposure. The four rainfall variables performed slightly better than seasonal rainfall alone in rolling-origin evaluation, although the difference was small and not statistically significant. The clearest agricultural response was observed in the detrended sorghum harvested-area ratio, while yield responses were weaker and the sesame results remained uncertain after data-quality screening.

At regional scale, daily rainfall indicators can help identify seasons in which surface drying and agricultural exposure may be higher. DRSRI provides an annual summary, but its component variables are still needed to identify the main rainfall constraint in each season. Future work should apply these indicators within mapped cropland and link them with independent soil-moisture observations, crop management records, and field-based land-condition data.

6. Declarations

Ethical approval

Not applicable.

Consent to participate

Not applicable.

Consent to publish

Not applicable.

Plant guidelines

This study did not involve the collection, cultivation, or experimental use of any plant material. Sorghum and sesame data were obtained as pre-existing annual administrative crop statistics from the Gedaref State Ministry of Production and Economic Resources and the Mechanized Farming Corporation. No plant specimens were collected, propagated, or handled by the authors, and no plant collection permits were required.

Competing interests

The authors declare no competing interests.

Funding

This research received no external funding.

Author contributions

Mohamed Abaker: Data curation and formal analysis. Jamal Elfaki: Conceptualization, methodology, supervision, writing—original draft, and writing, review and editing. Both authors read and approved the final version of the manuscript.

Data availability

The derived datasets and analytical code supporting the findings of this study are available from the corresponding author upon reasonable request. The original administrative crop records remain subject to the data-access conditions of the source institutions.

Supplementary information

The online version contains supplementary material comprising the annual indicator series, the CHIRPS evaluation data and statistics, and the full PCA, temporal-holdout, rolling-origin, crop-correlation, compound-event, trend, and sensitivity results (Supplementary Tables S1–S16).

References

Abdalla, S.A.M.E.H., 2022. Analysis of value chain and competitiveness of sesame crop in Gadarif State, Sudan. Doctoral dissertation, Sudan University of Science and Technology, Khartoum, Sudan.

Abdi, H., Williams, L.J., 2010. Principal component analysis. Wiley Interdisciplinary Reviews: Computational Statistics, 2, 433–459. https://doi.org/10.1002/wics.101

Alexander, L.V., Zhang, X., Peterson, T.C., Caesar, J., Gleason, B., Klein Tank, A.M.G., Haylock, M., Collins, D., Trewin, B., Rahimzadeh, F., Tagipour, A., Rupa Kumar, K., Revadekar, J., Griffiths, G., Vincent, L., Stephenson, D.B., Burn, J., Aguilar, E., Brunet, M., Taylor, M., New, M., Zhai, P., Rusticucci, M., Vazquez-Aguirre, J.L., 2006. Global observed changes in daily climate extremes of temperature and precipitation. Journal of Geophysical Research: Atmospheres, 111, D05109. https://doi.org/10.1029/2005JD006290

Allen, R.G., Pereira, L.S., Raes, D., Smith, M., 1998. Crop evapotranspiration: Guidelines for computing crop water requirements. FAO Irrigation and Drainage Paper No. 56. Food and Agriculture Organization of the United Nations, Rome.

Arsenault, K.R., Shukla, S., Hazra, A., Getirana, A., McNally, A., Kumar, S.V., Koster, R.D., Peters-Lidard, C.D., Zaitchik, B.F., Badr, H., Jung, H.C., Narapusetty, B., Navari, M., Wang, S., Mocko, D.M., Funk, C., Harrison, L., Husak, G.J., Adoum, A., Galu, G., Magadzire, T., Roningen, J., Shaw, M., Eylander, J., Bergaoui, K., McDonnell, R.A., Verdin, J.P., 2020. The NASA hydrological forecast system for food and water security applications. Bulletin of the American Meteorological Society, 101, E1007–E1025. https://doi.org/10.1175/BAMS-D-18-0264.1

Ati, O.F., Stigter, C.J., Oladipo, E.O., 2002. A comparison of methods to determine the onset of the growing season in northern Nigeria. International Journal of Climatology, 22, 731–742. https://doi.org/10.1002/joc.712

Babiker, E.H., 2010. The factors affecting sesame production in Gedarif Area, Sudan. Master's thesis, Sudan Academy of Sciences, Khartoum, Sudan.

Bartlett, M.S., 1954. A note on the multiplying factors for various chi-square approximations. Journal of the Royal Statistical Society: Series B (Methodological), 16, 296–298. https://doi.org/10.1111/j.2517-6161.1954.tb00174.x

Benjamini, Y., Hochberg, Y., 1995. Controlling the false discovery rate: A practical and powerful approach to multiple testing. Journal of the Royal Statistical Society: Series B (Methodological), 57, 289–300. https://doi.org/10.1111/j.2517-6161.1995.tb02031.x

Blokhuis, W.A., 1993. Vertisols in the central clay plain of the Sudan. Wageningen Agricultural University, Wageningen.

Bronswijk, J.J.B., 1988. Modeling of water balance, cracking and subsidence of clay soils. Journal of Hydrology, 97, 199–212. https://doi.org/10.1016/0022-1694(88)90115-1

Cattell, R.B., 1966. The scree test for the number of factors. Multivariate Behavioral Research, 1, 245–276. https://doi.org/10.1207/s15327906mbr0102_10

Dinku, T., Ceccato, P., Grover-Kopec, E., Lemma, M., Connor, S.J., Ropelewski, C.F., 2007. Validation of satellite rainfall products over East Africa's complex topography. International Journal of Remote Sensing, 28, 1503–1526. https://doi.org/10.1080/01431160600954688

Dorigo, W., Wagner, W., Albergel, C., Albrecht, F., Balsamo, G., Brocca, L., Chung, D., Ertl, M., Forkel, M., Gruber, A., Haas, E., Hamer, P.D., Hirschi, M., Ikonen, J., de Jeu, R., Kidd, R., Lahoz, W., Liu, Y.Y., Miralles, D., Mistelbauer, T., Nicolai-Shaw, N., Parinussa, R., Pratola, C., Reimer, C., van der Schalie, R., Seneviratne, S.I., Smolander, T., Lecomte, P., 2017. ESA CCI Soil Moisture for improved Earth system understanding: State-of-the-art and future directions. Remote Sensing of Environment, 203, 185–215. https://doi.org/10.1016/j.rse.2017.07.001

Dunning, C.M., Black, E.C.L., Allan, R.P., 2016. The onset and cessation of seasonal rainfall over Africa. Journal of Geophysical Research: Atmospheres, 121, 11405–11424. https://doi.org/10.1002/2016JD025428

Efron, B., Tibshirani, R.J., 1993. An introduction to the bootstrap. Chapman & Hall, New York.

Ek, M.B., Mitchell, K.E., Lin, Y., Rogers, E., Grunmann, P., Koren, V., Gayno, G., Tarpley, J.D., 2003. Implementation of Noah land surface model advances in the National Centers for Environmental Prediction operational mesoscale Eta model. Journal of Geophysical Research: Atmospheres, 108, 8851. https://doi.org/10.1029/2002JD003296

Entekhabi, D., Njoku, E.G., O'Neill, P.E., Kellogg, K.H., Crow, W.T., Edelstein, W.N., Entin, J.K., Goodman, S.D., Jackson, T.J., Johnson, J., Kimball, J., Piepmeier, J.R., Koster, R.D., Martin, N., McDonald, K.C., Moghaddam, M., Moran, S., Reichle, R., Shi, J.C., Spencer, M.W., Thurman, S.W., Tsang, L., Van Zyl, J., 2010. The Soil Moisture Active Passive (SMAP) mission. Proceedings of the IEEE, 98, 704–716. https://doi.org/10.1109/JPROC.2010.2043918

Funk, C., Peterson, P., Landsfeld, M., Pedreros, D., Verdin, J., Shukla, S., Husak, G., Rowland, J., Harrison, L., Hoell, A., Michaelsen, J., 2015. The Climate Hazards Infrared Precipitation with Stations: A new environmental record for monitoring extremes. Scientific Data, 2, 150066. https://doi.org/10.1038/sdata.2015.66

Gebrechorkos, S.H., Hülsmann, S., Bernhofer, C., 2019. Long-term trends in rainfall and temperature using high-resolution climate datasets in East Africa. Scientific Reports, 9, 11376. https://doi.org/10.1038/s41598-019-47933-8

Gedaref State Ministry of Production and Economic Resources, n.d.-a. Gedaref monthly rainfall records, 1982–2020 [Unpublished administrative dataset]. Gedaref, Sudan.

Gedaref State Ministry of Production and Economic Resources, n.d.-b. Annual sorghum planted area, productive area, and production records for Gedaref State, 1982–2020 [Unpublished administrative dataset]. Mechanized Farming Corporation, Gedaref, Sudan.

Gedaref State Ministry of Production and Economic Resources, n.d.-c. Annual sesame planted area, productive area, and production records for Gedaref State, 1982–2020 [Unpublished administrative dataset]. Mechanized Farming Corporation, Gedaref, Sudan.

Gruber, A., Scanlon, T., van der Schalie, R., Wagner, W., Dorigo, W., 2019. Evolution of the ESA CCI Soil Moisture climate data records and their underlying merging methodology. Earth System Science Data, 11, 717–739. https://doi.org/10.5194/essd-11-717-2019

Gruber, A., De Lannoy, G., Albergel, C., Al-Yaari, A., Brocca, L., Calvet, J.-C., Colliander, A., Cosh, M., Crow, W., Dorigo, W., Draper, C., Hirschi, M., Kerr, Y., Konings, A., Lahoz, W., McColl, K., Montzka, C., Muñoz-Sabater, J., Peng, J., Reichle, R., Richaume, P., Rüdiger, C., Scanlon, T., van der Schalie, R., Wigneron, J.-P., Wagner, W., 2020. Validation practices for satellite soil moisture retrievals: What are (the) errors? Remote Sensing of Environment, 244, 111806. https://doi.org/10.1016/j.rse.2020.111806

Gupta, H.V., Kling, H., Yilmaz, K.K., Martinez, G.F., 2009. Decomposition of the mean squared error and NSE performance criteria: Implications for improving hydrological modelling. Journal of Hydrology, 377, 80–91. https://doi.org/10.1016/j.jhydrol.2009.08.003

Hamed, K.H., Rao, A.R., 1998. A modified Mann–Kendall trend test for autocorrelated data. Journal of Hydrology, 204, 182–196. https://doi.org/10.1016/S0022-1694(97)00125-X

Hastie, T., Tibshirani, R., Friedman, J., 2009. The elements of statistical learning: Data mining, inference, and prediction, 2nd ed. Springer, New York. https://doi.org/10.1007/978-0-387-84858-7

Hillel, D., 1998. Environmental soil physics. Academic Press, San Diego.

Horn, J.L., 1965. A rationale and test for the number of factors in factor analysis. Psychometrika, 30, 179–185. https://doi.org/10.1007/BF02289447

Ibrahim, E.J., Muhieldeen, O.A., 2018. Review of sesame crop harvesting in Sudan: Trials, difficulties and future prospects. SUST Journal of Agricultural and Veterinary Sciences, 19, 58–67. http://repository.sustech.edu/handle/123456789/21637

IPCC, 2022. Climate change 2022: Impacts, adaptation and vulnerability. Contribution of Working Group II to the Sixth Assessment Report of the Intergovernmental Panel on Climate Change. Cambridge University Press, Cambridge and New York. https://doi.org/10.1017/9781009325844

Jolliffe, I.T., 2002. Principal component analysis, 2nd ed. Springer, New York. https://doi.org/10.1007/b98835

Jolliffe, I.T., Cadima, J., 2016. Principal component analysis: A review and recent developments. Philosophical Transactions of the Royal Society A: Mathematical, Physical and Engineering Sciences, 374, 20150202. https://doi.org/10.1098/rsta.2015.0202

Kaiser, H.F., 1974. An index of factorial simplicity. Psychometrika, 39, 31–36. https://doi.org/10.1007/BF02291575

Kendall, M.G., 1975. Rank correlation methods, 4th ed. Charles Griffin, London.

Kling, H., Fuchs, M., Paulin, M., 2012. Runoff conditions in the upper Danube basin under an ensemble of climate change scenarios. Journal of Hydrology, 424–425, 264–277. https://doi.org/10.1016/j.jhydrol.2012.01.011

Legates, D.R., McCabe, G.J., 1999. Evaluating the use of goodness-of-fit measures in hydrologic and hydroclimatic model validation. Water Resources Research, 35, 233–241. https://doi.org/10.1029/1998WR900018

Lobell, D.B., Burke, M.B., 2010. On the use of statistical models to predict crop yield responses to climate change. Agricultural and Forest Meteorology, 150, 1443–1452. https://doi.org/10.1016/j.agrformet.2010.07.008

Lobell, D.B., Schlenker, W., Costa-Roberts, J., 2011. Climate trends and global crop production since 1980. Science, 333, 616–620. https://doi.org/10.1126/science.1204531

Mann, H.B., 1945. Nonparametric tests against trend. Econometrica, 13, 245–259. https://doi.org/10.2307/1907187

Marteau, R., Sultan, B., Moron, V., Alhassane, A., Baron, C., Traoré, S.B., 2011. The onset of the rainy season and farmers' sowing strategy for pearl millet cultivation in southwest Niger. Agricultural and Forest Meteorology, 151, 1356–1369. https://doi.org/10.1016/j.agrformet.2011.05.018

McKee, T.B., Doesken, N.J., Kleist, J., 1993. The relationship of drought frequency and duration to time scales. In: Proceedings of the Eighth Conference on Applied Climatology, Anaheim, California, pp. 179–184. American Meteorological Society, Boston, MA.

McNally, A., Shukla, S., Arsenault, K.R., Wang, S., Peters-Lidard, C.D., Verdin, J.P., 2017. A land data assimilation system for sub-Saharan Africa food and water security applications. Scientific Data, 4, 170012. https://doi.org/10.1038/sdata.2017.12

Mishra, A.K., Singh, V.P., 2010. A review of drought concepts. Journal of Hydrology, 391, 202–216. https://doi.org/10.1016/j.jhydrol.2010.07.012

Nash, J.E., Sutcliffe, J.V., 1970. River flow forecasting through conceptual models. Part I: A discussion of principles. Journal of Hydrology, 10, 282–290. https://doi.org/10.1016/0022-1694(70)90255-6

Nicholson, S.E., 2017. Climate and climatic variability of rainfall over eastern Africa. Reviews of Geophysics, 55, 590–635. https://doi.org/10.1002/2016RG000544

O'Brien, R.M., 2007. A caution regarding rules of thumb for variance inflation factors. Quality & Quantity, 41, 673–690. https://doi.org/10.1007/s11135-006-9018-6

Oliver, J.E., 1980. Monthly precipitation distribution: A comparative index. The Professional Geographer, 32, 300–309. https://doi.org/10.1111/j.0033-0124.1980.00300.x

Palmer, W.C., 1965. Meteorological drought. U.S. Weather Bureau Research Paper No. 45. U.S. Weather Bureau, Washington, DC.

Pettitt, A.N., 1979. A non-parametric approach to the change-point problem. Journal of the Royal Statistical Society: Series C (Applied Statistics), 28, 126–135. https://doi.org/10.2307/2346729

Rockström, J., Barron, J., Fox, P., 2002. Rainwater management for increased productivity among smallholder farmers in drought-prone environments. Physics and Chemistry of the Earth, Parts A/B/C, 27, 949–959. https://doi.org/10.1016/S1474-7065(02)00098-0

Rockström, J., 2003. Water for food and nature in drought-prone tropics: Vapour shift in rain-fed agriculture. Philosophical Transactions of the Royal Society B: Biological Sciences, 358, 1997–2009. https://doi.org/10.1098/rstb.2003.1400

Rockström, J., Barron, J., Fox, P., Falkenmark, M., 2010. Managing water in rainfed agriculture: The need for a paradigm shift. Agricultural Water Management, 97, 543–550. https://doi.org/10.1016/j.agwat.2009.09.009

Rodell, M., Houser, P.R., Jambor, U., Gottschalck, J., Mitchell, K., Meng, C.-J., Arsenault, K., Cosgrove, B., Radakovich, J., Bosilovich, M., Entin, J.K., Walker, J.P., Lohmann, D., Toll, D., 2004. The Global Land Data Assimilation System. Bulletin of the American Meteorological Society, 85, 381–394. https://doi.org/10.1175/BAMS-85-3-381

Schlenker, W., Lobell, D.B., 2010. Robust negative impacts of climate change on African agriculture. Environmental Research Letters, 5, 014010. https://doi.org/10.1088/1748-9326/5/1/014010

Sen, P.K., 1968. Estimates of the regression coefficient based on Kendall's tau. Journal of the American Statistical Association, 63, 1379–1389. https://doi.org/10.1080/01621459.1968.10480934

Seneviratne, S.I., Corti, T., Davin, E.L., Hirschi, M., Jaeger, E.B., Lehner, I., Orlowsky, B., Teuling, A.J., 2010. Investigating soil moisture–climate interactions in a changing climate: A review. Earth-Science Reviews, 99, 125–161. https://doi.org/10.1016/j.earscirev.2010.02.004

Sivakumar, M.V.K., 1988. Predicting rainy season potential from the onset of rains in southern Sahelian and Sudanian climatic zones of West Africa. Agricultural and Forest Meteorology, 42, 295–305. https://doi.org/10.1016/0168-1923(88)90039-1

Sivakumar, M.V.K., 1992. Empirical analysis of dry spells for agricultural applications in West Africa. Journal of Climate, 5, 532–539. https://doi.org/10.1175/1520-0442(1992)005<0532:EAODSF>2.0.CO;2

Stern, R.D., Dennett, M.D., Garbutt, D.J., 1981. The start of the rains in West Africa. Journal of Climatology, 1, 59–68. https://doi.org/10.1002/joc.3370010107

Stone, M., 1974. Cross-validatory choice and assessment of statistical predictions. Journal of the Royal Statistical Society: Series B (Methodological), 36, 111–147. https://doi.org/10.1111/j.2517-6161.1974.tb00994.x

Sulieman, H.M., Buchroithner, M.F., 2009. Degradation and abandonment of mechanized rain-fed agricultural land in the southern Gadarif region, Sudan: The local farmers' perception. Land Degradation & Development, 20, 199–209. https://doi.org/10.1002/ldr.894

Sultan, B., Roudier, P., Quirion, P., Alhassane, A., Muller, B., Dingkuhn, M., Ciais, P., Guimberteau, M., Traoré, S., Baron, C., 2013. Assessing climate change impacts on sorghum and millet yields in the Sudanian and Sahelian savannas of West Africa. Environmental Research Letters, 8, 014040. https://doi.org/10.1088/1748-9326/8/1/014040

United Nations Industrial Development Organization, 2017. Upgrading the Sudanese sesame seeds value chain (Project No. 160177). United Nations Industrial Development Organization, Vienna.

Usman, M.T., Reason, C.J.C., 2004. Dry spell frequencies and their variability over southern Africa. Climate Research, 26, 199–211. https://doi.org/10.3354/cr026199

Usman, M., Razzaq, M., Khan, R.A.R., Rehman, M.A., Ali, M.M., Gull, S., Yousef, A.F., Adnan, M., Ercisli, S., Golokhvast, K.S., 2022. Factors affecting postharvest losses of sesame (Sesamum indicum L.) and their mitigation strategies. Agronomy, 12, 2470. https://doi.org/10.3390/agronomy12102470

Wilding, L.P., Tessier, D., 1988. Genesis of Vertisols: Shrink–swell phenomena. In: Wilding, L.P., Puentes, R. (eds.), Vertisols: Their distribution, properties, classification and management. Texas A&M University Printing Center, College Station, TX, pp. 55–81.

Wilks, D.S., 2011. Statistical methods in the atmospheric sciences, 3rd ed. Academic Press, Oxford.

Yue, S., Pilon, P., Phinney, B., Cavadias, G., 2002. The influence of autocorrelation on the ability to detect trend in hydrological series. Hydrological Processes, 16, 1807–1829. https://doi.org/10.1002/hyp.1095

Yue, S., Wang, C.Y., 2004. The Mann–Kendall test modified by effective sample size to detect trend in serially correlated hydrological series. Water Resources Management, 18, 201–218. https://doi.org/10.1023/B:WARM.0000043140.61082.60

Zargar, A., Sadiq, R., Naser, B., Khan, F.I., 2011. A review of drought indices. Environmental Reviews, 19, 333–349. https://doi.org/10.1139/a11-013

Zhang, X., Alexander, L., Hegerl, G.C., Jones, P.D., Tank, A.K., Peterson, T.C., Trewin, B., Zwiers, F.W., 2011. Indices for monitoring changes in extremes based on daily temperature and precipitation data. Wiley Interdisciplinary Reviews: Climate Change, 2, 851–870. https://doi.org/10.1002/wcc.147

Zscheischler, J., Westra, S., van den Hurk, B.J.J.M., Ward, P.J., Pitman, A., AghaKouchak, A., Bresch, D.N., Leonard, M., Wahl, T., Zhang, X., 2018. Future climate risk from compound events. Nature Climate Change, 8, 469–477. https://doi.org/10.1038/s41558-018-0156-3

Zscheischler, J., Martius, O., Westra, S., Bevacqua, E., Raymond, C., Horton, R.M., van den Hurk, B., AghaKouchak, A., Jézéquel, A., Mahecha, M.D., Maraun, D., Ramos, A.M., Ridder, N.N., Thiery, W., Vignotto, E., 2020. A typology of compound weather and climate events. Nature Reviews Earth & Environment, 1, 333–347. https://doi.org/10.1038/s43017-020-0060-z

Supplementary Files

This is a list of supplementary files associated with this preprint. Click to download.

- TableS1Annualindicators19822020.csv
- TableS6Temporalholdoutcomparison.csv
- TableS8PairedbootstrapRMSE.csv
- TableS9Primarycropcorrelations.csv
- TableS2CHIRPSstationevaluation.csv
- SupplementaryMaterialDiscoverSoil.xlsx
- TableS13Onsetsensitivity.csv
- TableS4PCAcoefficientsanddiagnostics.csv
- TableS5Parallelanalysis.csv
- TableS11Compoundresponses.csv
- TableS15Indexsensitivity.csv
- TableS12Compoundsensitivity.csv
- TableS16MonthlyCHIRPSandstationrainfall.csv
- TableS10Cropsensitivity.csv
- TableS14Trendresults.csv